# Hydrothermal synthesis, structure and luminescent properties of one-dimensional lanthanide benzenedicarboxylates, $[M(NO_3)M_2(C_{12}H_8N_2)_2][(C_8H_4O_4)_4]\cdot H_2O$, (M = La, Pr), possessing infinite M–O–M linkages†

**A. Thirumurugan[a] and Srinivasan Natarajan*[b]**

*Received 18th July 2005, Accepted 31st August 2005*
*First published as an Advance Article on the web 23rd September 2005*
**DOI: 10.1039/b510146h**

A hydrothermal reaction of a mixture of $M(NO_3)_3$, 1,2-dicyanobenzene, 1,2-benzenedicarboxylic acid (1,2-BDC), 1,10-phenanthroline and piperazine gave rise to a new compound, $[M(NO_3)M_2(C_{12}H_8N_2)_2][(C_8H_4O_4)_4]\cdot H_2O$, (M = La, **I** and Pr, **II**). The structure is built up from the connectivity of $MO_n$ polyhedra by sharing an edge or face. The metal atoms are coordinated by 1,10-phenanthroline or nitrate groups along with the phthalates resulting in an infinite one-dimensional M–O–M chain. The crystal structure is stabilized by π···π and CH···π interactions. Our preliminary investigations of the $Eu^{3+}/Tb^{3+}$ doped samples (in place of $La^{3+}$), indicate that interesting red/pink or green luminescence can obtained by excitation at 252 nm. The luminescence behavior probably results from the ligand-sensitized metal-centered emission.

## Introduction

Metal–organic framework (MOF) structures constitute an important family of compounds with tremendous potential in the area of catalysis, sorption, non-linear optics, luminescence *etc*.[1–10] Most of the MOF structures are built up from discrete metal polyhedra or isolated small clusters connected by organic linkers, giving rise to structures of varying dimensionality.[10–13] In many cases, benzenedicarboxylates with angles of 60, 120 and 180° suspended between the two acid groups act as a very good linker. The variations in the linking ability of the carboxylate groups can also be tuned in designing new MOF structures.[14,15] Recently, the use of two different benzene dicarboxylic acids has been shown to give rise to a new type of hybrid structures.[13,16] The use of inorganic and organic acids in the design and synthesis of MOF structures have been rare.[17] In addition, the interest in the study of metal–organic hybrid compounds has been enhanced by the report of red and green emission in $Eu^{3+}$ and $Tb^{3+}$ doping by Férey and coworkers. We have been interested in the study of rare-earth benzene dicarboxylates, especially for their variety in the coordination geometries and also interesting properties such as luminescence.[18–29] During the course of our study, we have now prepared a new metal–organic framework of the formula, $[M(NO_3)M_2(C_{12}H_8N_2)_2][(C_8H_4O_4)_4]\cdot H_2O$, (M = La, **I** and Pr, **II**). The structures of both the compounds are identical and are formed by three different coordination polyhedra of $M^{3+}$ ions (M = La and Pr) connected by phthalate and nitrate anions with 1,10-phenanthroline acting as the secondary ligand. The edge- and face-sharing connectivity between the polyhedral units gives rise to M–O–M infinite one-dimensional chains. The presence of both the nitrate and phthalate anions in the structures is noteworthy. We have also doped $Eu^{3+}$ and $Tb^{3+}$ (2 and 4 mol%) in place of $La^{3+}$ to investigate the luminescence properties. In this paper, we present the synthesis, structure and luminescent properties of all the compounds.

## Experimental

### Synthesis and initial characterization

In a typical synthesis, 1 mM of $M(NO_3)_3$ (0.325 g for La and 0.327 g for Pr) was dissolved in 5 ml of MilliQ water. To this, 0.128 g (1 mM) of 1,2-dicyanobenzene [$NC(C_6H_4)CN$], 0.169 g (1 mM) of phthalic acid, [$HOOC(C_6H_4)COOH$], (1,2-BDC) and 0.199 g (1 mM) of 1,10-phenanthroline were added under continuous stirring followed by the addition of 0.087 g (1 mM) of piperazine. The mixture was homogenized for 30 min at room temperature. The final mixture with the composition, $M(NO_3)_3$ : $1,2(NC)_2C_6H_4$ : 1,2-BDC : 1.10-phenanthroline : piperazine : $278H_2O$, was sealed in a 23 ml PTFE-lined acid digestion bomb and heated at 180 °C for 72 h under autogeneous pressure. The Eu (2 mol%, **Ia**; 4 mol%, **Ib**) and Tb (2 mol%, **Ic**; 4 mol%, **Id**) substituted compounds were also prepared employing similar synthesis procedure using $Eu_2(C_2O_4)_3$ and $Tb_2(CO_3)_3$ as the source of Eu and Tb. In all cases, large quantities of rod-like single crystals were obtained. The product was filtered under vacuum and dried at ambient temperature. Though the synthesis mixture contained 1,2-dicyanobenzene (1,2-DCB) as one of the reactant, the final product contained only benzene-1,2-dicarboxylic acid (phthalic acid). It is likely that 1,2-DCB would have undergone hydrolysis during the hydrothermal reaction to give rise to the phthalic acid. Similar hydrolysis of 1,2-DCB has been

[a]*Chemistry and Physics of Materials Unit, Jawaharlal Nehru Centre for Advanced Scientific Research, Jakkur P.O., Bangalore, 560064, India. E-mail: snatarajan@sscu.iisc.ernet.in*
[b]*Framework Solids Laboratory, Solid State and Structural Chemistry Unit, Indian Institute of Science, Bangalore-560012, India*
† Electronic supplementary information (ESI) available: Packing diagrams, photoluminescence spectra, TGA, XRD, IR spectra and crystallographic data. See http://dx.doi.org/10.1039/b510146h

 

observed earlier.[13,30–32] The use of pure 1,2-BDC in the synthesis mixture also produced the title compounds, but in powder form. We could obtain single crystals, suitable for structure determination by single crystal X-ray diffraction, by the use of a 1 : 1 mixture of 1,2-BDC and 1,2-DCB. The exact role of 1,2-DCB in the synthesis mixture is not clear. It is likely that the slow release of 1,2-BDC in the reaction mixture by the hydrolysis of 1,2-DCB would have resulted in the formation of single crystals. The initial characterizations were carried out using powder X-ray diffraction (XRD), thermogravimetric analysis (TGA) and infra-red (IR) spectroscopy. The powder XRD patterns were recorded on crushed single crystals in the $2\theta$ range 5–50° using Cu K$\alpha$ radiation. The XRD patterns indicated that the products were new materials; the patterns were entirely consistent with the simulated pattern generated from the single-crystal structure.

Thermogravimetric analysis (TGA, Metler-Toledo) was carried out in oxygen atmosphere (flow rate = 50 ml $min^{-1}$) in the temperature range 30 to 600 °C (heating rate = 5 °C $min^{-1}$). The studies show identical results for both the compounds with two weight losses. The initial weight loss of 6% in the range 170–280 °C corresponds to the loss of the lattice water and the nitrate group bound to the $M^{3+}$ ion (calc. 5.29 and 5.26% for **I** and **II**) and the second weight loss of 67.3% and 66.15% for **I** and **II** in the range 360–450 °C corresponds to the loss of the 1,10-phenanthroline and the phthalate groups (calc. 67.16% and 66.9% for **I** and **II**). The calcined samples were crystalline and the powder XRD lines matches well with the corresponding pure oxides. [JCPDS no.: 40-1284 ($La_2O_3$) and 42-1121 ($Pr_6O_{11}$)]

Infra-red (IR) spectroscopic studies have been carried out in the mid-IR region as a KBr pellet using Bruker IFS-66v spectrometer. The results indicate characteristic sharp lines with almost similar bands. Minor variations between the bands have been noticed between the compounds. The observed bands are: 3300–3600(s) $cm^{-1}$ $\nu_s$OH, 3059(w) $cm^{-1}$ $\nu_s(C–H)_{aromatic}$, 1714(m) $cm^{-1}$ $\nu_s$(C=O), 1605(w) $cm^{-1}$ $\delta_s H_2O$, 1535(s) $\nu$(N=O), 1425(s) $cm^{-1}$ $\delta_s$(COO), 1401(s) $cm^{-1}$ $\delta$(OH), 1132(m) $cm^{-1}$ $\delta_s$(NO), 1289–1294(s) $cm^{-1}$ $\delta_a$(NO) and $\delta$(CO), 1140(s) $cm^{-1}$ $\delta(CH_{aromatic})_{in\text{-}plane}$, 750(s) and 840(s) $cm^{-1}$ $\delta(CH_{aromatic})_{out\text{-}of\text{-}plane}$. Room temperature solid-state photoluminescence studies were carried out on powdered samples (Perkin-Elmer spectrometer (LS-55) with a single beam set-up was employed using a 50 W xenon lamp as the source and a photo-multiplier tube as the detector).

### Single crystal structure determination

A suitable single crystal of each compound was carefully selected under a polarizing microscope and glued to a thin glass fiber. Crystal structure determination by X-ray diffraction was performed on a Siemens Smart-CCD diffractometer equipped with a normal focus, 2.4 kW sealed tube X-ray source (Mo K$\alpha$ radiation, $\lambda$ = 0.71073 Å) operating at 40 kV and 40 mA. An empirical absorption correction based on symmetry equivalent reflections was applied using the SADABS program.[33] The structure was solved and refined using SHELXTL-PLUS suite of program.[34] All the hydrogen atoms of the carboxylic acids were initially located in the difference Fourier maps and for the final refinement the hydrogen atoms were placed in geometrically ideal positions and held in the riding mode. The hydrogen atoms of the water molecule were not located in the difference Fourier maps. Final refinement included atomic positions for all the atoms, anisotropic thermal parameters for all the non-hydrogen atoms and isotropic thermal parameters for all the hydrogen atoms. Full-matrix least-squares refinement against $|F|^2$, was carried out using the SHELXTL-PLUS[34] suite of programs. Details of the structure solution and final refinements for **I** and **II** are given in Table 1. Selected bond distances are listed in Table 2.

## Results and discussion

Both **I** and **II** are iso-structural and have 85 non-hydrogen atoms in the asymmetric unit. There are three crystallographically distinct $M^{3+}$ ions and four phthalate anions. The $M^{3+}$ ions are connected to four phthalate anions, a nitrate anion and two 1,10-phenanthroline ligands. The four phthalate anions {acid-1-[C(41)–(C48), acid-2-[C(51)–(C58)], acid-3-[C(61)–(C68)] and acid-4-[C(71)–(C78)]} can be classified into three different types based on their coordination modes with the metal atoms (Fig. 1). The metal atom, M(1), is surrounded by ten oxygen atoms and has a distorted bicapped square antiprism environment ($MO_{10}$, CN = 10). Among the ten, two oxygen atoms [O(9) and O(10)] are from the nitrate group and the remaining 8 oxygens are from the four phthalate anions. Five oxygen atoms, O(1), O(3), O(5), O(6) and O(7) have $\mu_3$ connections linking two metal centres and a carbon atom.

**Table 1** Crystal data and structure refinement parameters for **I** and **II**, $[M(NO_3)M_2(C_{12}H_8N_2)_2][(C_8H_4O_4)_4]\cdot H_2O$ (M = La, Pr)

| Structure parameter | La | Pr |
|---|---|---|
| Empirical formula | $C_{112}H_{64}La_6O_{39}N_{10}$ | $C_{112}H_{64}Pr_6O_{39}N_{10}$ |
| Formula weight | 3007.21 | 3019.23 |
| Crystal system | Triclinic | Triclinic |
| Space group | $P\bar{1}$ (no. 2) | $P\bar{1}$, (no. 2) |
| $a$/Å | 12.8146(2) | 12.7564(1) |
| $b$/Å | 13.1192(2) | 13.1300(1) |
| $c$/Å | 17.5359(2) | 17.5490(3) |
| $\alpha$/° | 89.1100 | 89.4760(10) |
| $\beta$/° | 79.8090(10) | 79.5100 |
| $\gamma$/° | 65.9370(10) | 65.9120(10) |
| $V$/Å$^3$ | 2644.16(7) | 2631.54(6) |
| $Z$ | 1 | 1 |
| $D_{(calc)}$/g $cm^{-3}$ | 1.889 | 1.905 |
| $\mu$/$mm^{-1}$ | 2.465 | 2.819 |
| $\lambda$ (Mo K$\alpha$)/Å | 0.71073 | 0.71073 |
| $F$(000) | 1460 | 1472 |
| $2\theta$ range/° | 2.4–46.6 | 2.4–46.4 |
| Total data collected | 11 111 | 10 904 |
| Unique data | 7456 | 7345 |
| Observed data [$I > 2\sigma(I)$] | 6019 | 5496 |
| $R_{merg}$ | 0.0340 | 0.0324 |
| $R$ indexes [$I > 2\sigma(I)$] | $R_1$ = 0.0330[a]; w$R_2$ = 0.0701[b] | $R_1$ = 0.0339[a]; w$R_2$ = 0.0585[b] |
| $R$ indexes [all data] | $R_1$ = 0.0453[a]; w$R_2$ = 0.0741[b] | $R_1$ = 0.0580[a]; w$R_2$ = 0.0662[b] |
| Largest difference map peak and hole/e Å$^{-3}$ | 0.74 and −1.28 | 0.56 and −0.66 |

[a] $R_1 = \Sigma||F_o| - |F_c||/\Sigma|F_o|$; [b] $wR_2 = \{\Sigma [w(F_o^2 - F_c^2)^2]/\Sigma[w(F_o^2)^2]\}^{1/2}$. $w = 1/[\sigma^2(F_o)^2 + (aP)^2 + bP]$, $P = [\max.(F_o^2,0) + 2(F_c)^2]/3$, where $a$ = 0.0131 and $b$ = 0.0 La and $a$ = 0.0 and $b$ = 0.0 for Pr.

**Table 2** Selected bond distances in **I** and **II**, $[M(NO_3)M_2(C_{12}H_8N_2)_2][(C_8H_4O_4)_4]\cdot H_2O$ (M = La, Pr)

| | Distance/Å | | | Distance/Å | | | Distance/Å | |
|---|---|---|---|---|---|---|---|---|
| Bond | La | Pr | Bond | La | Pr | Bond | La | Pr |
| M(1)–O(1) | 2.693(3) | 2.692(4) | M(2)–O(1) | 2.544(3) | 2.498(4) | M(3)–O(3) | 2.598(3) | 2.575(4) |
| M(1)–O(2) | 2.550(4) | 2.507(4) | M(2)–O(7) | 2.657(3) | 2.630(4) | M(3)–O(5) | 2.586(3) | 2.546(4) |
| M(1)–O(3) | 2.639(3) | 2.601(4) | M(2)–O(11) | 2.532(4) | 2.480(4) | M(3)–O(6) | 2.655(3) | 2.632(4) |
| M(1)–O(4) | 2.554(4) | 2.506(4) | M(2)–O(12) | 2.555(4) | 2.499(4) | M(3)–O(15) | 2.591(4) | 2.537(4) |
| M(1)–O(5) | 2.586(3) | 2.553(4) | M(2)–O(12)#1[a] | 2.498(4) | 2.456(4) | M(3)–O(16) | 2.562(4) | 2.521(4) |
| M(1)–O(6) | 2.547(4) | 2.506(4) | M(2)–O(13) | 2.571(4) | 2.525(5) | M(3)–O(17) | 2.699(4) | 2.678(4) |
| M(1)–O(7) | 2.581(3) | 2.546(4) | M(2)–N(1) | 2.703(5) | 2.664(5) | M(3)–O(18) | 2.729(4) | 2.696(4) |
| M(1)–O(8) | 2.567(4) | 2.536(4) | M(2)–N(2) | 2.747(5) | 2.702(5) | M(3)–O(18)#2[a] | 2.535(3) | 2.510(3) |
| M(1)–O(9) | 2.609(4) | 2.564(5) | | | | M(3)–N(3) | 2.708(4) | 2.662(5) |
| M(1)–O(10) | 2.631(4) | 2.590(4) | | | | M(3)–N(4) | 2.707(4) | 2.670(5) |

[a] Symmetry transformations used to generated equivalent atoms: #1 $-x,-y+1,-z+1$ #2 $-x+1,-y,-z$

M(2) is coordinated by six oxygen atoms and two nitrogen atoms and has a distorted dodecahedral environment ($MO_6N_2$, CN = 8). The two nitrogen atoms [N(1) and N(2)] are from the 1,10-phenanthroline ligand and the six oxygen atoms are from the four phthalate anions. Three oxygen atoms, O(1), O(7) and O(12)] have $\mu_3$ connectivity. M(3) is coordinated by eight oxygen atoms and two nitrogen atoms and has a distorted bicapped square anti-prism environment ($MO_8N_2$, CN = 10). The two nitrogen atoms [N(3) and N(4)] are from the 1,10-phenanthroline ligand and the eight oxygen atoms are from the four phthalate anions. Four oxygen atoms, O(3), O(5), O(6) and O(18) have $\mu_3$ connectivity. The M–O bonds have distances in the range 2.456(4)–2.729(4) Å and the M–N bonds have distances in the range 2.662(5)–2.747(5) Å for **I** and **II**. The O–M–O bond angles are in the range 48.66(11)–167.15(12)° for **I** and **II**. We have obtained all the coordination distances for the $MO_n$ polyhedra by assuming the typical M–O distances in the range 2.4–2.8 Å.

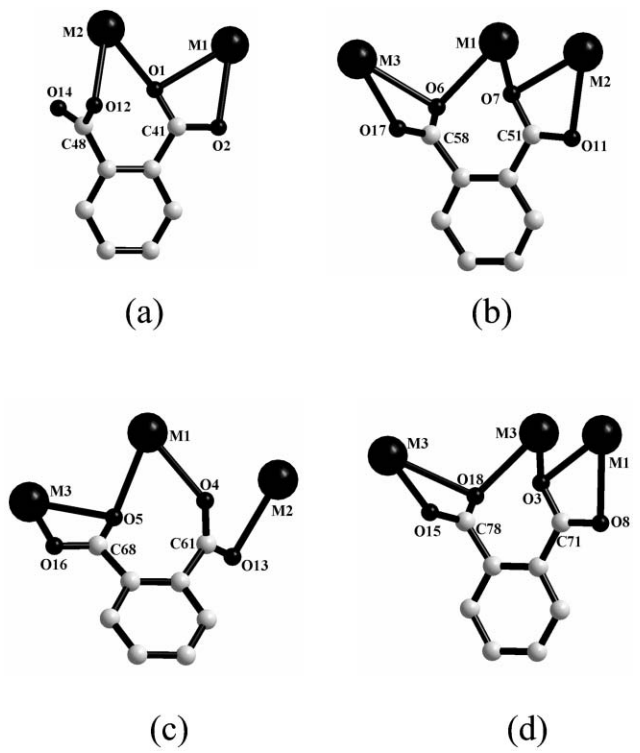


**Fig. 1** The various coordination modes of the phthalate anions observed in **I** and **II**. (a) acid 1, (b) acid 2, (c) acid 3 and (d) acid 4.

The structure of **I** and **II** can be explained by considering smaller building units. Thus, two $M(2)^{3+}$ ions are connected through two $\mu_3$ oxygen atoms [O(12)], from two different phthalate anions (both are acid 1) to form an edge-shared $M_2O_{12}N_4$ dimer. Similarly, two $M(3)^{3+}$ ions are connected through two $\mu_3$ oxygen atoms [O(18)], from two different phthalate anions (both are acid 4) to form an edge-shared $M_2O_{16}N_4$ dimer (Fig. 2a). The two dimers M(2) and M(3), are independently connected to each other by the acid 2 and acid 3 (Fig. 2b). In addition, the M(2) and M(3) dimers are also linked to M(1) by $\mu_3$ oxygen atoms. Thus, O(1) and O(7) connects the M(2) dimer with M(1) by sharing the edge, whereas O(3), O(5) and O(6) atoms connects the M(3) dimer with M(1) by sharing the face resulting in a head–tail type of arrangement. [(M(2)-dimer as the head and M(3)-dimer as the tail or *vice versa*] (Fig. 2a) The arrangement of the polyhedra gives rise to an infinite one-dimensional M–O–M chain structure decorated with phthalates, nitrates and 1,10-phenanthroline ligands as shown in Figs. 2b and 2c.

The structural stability in a low-dimensional structure is, in general, derived from weak non-covalent interactions. In the present case, we find $\pi\cdots\pi$ and $CH\cdots\pi$ interactions dominate and probably lend stability to the structure. The $\pi\cdots\pi$ interactions can be classified into three different types: acid–acid, 1,10-phenanthroline–acid and 1,10-phenanthroline–1,10-phenanthroline as shown in Fig. 3. Based on the classification, we find the centroid-to-centroid distances between all the participating aromatic rings to be in the range 3.622–3.716 Å and the dihedral angles to be in the range 0–5.7°. The CH to centroid distances are in the range 2.785–3.399 Å and the angles in the range 87.77–153.14° for **I** and **II**.

The role of $\pi\cdots\pi$ interactions in the stability and structure of supramolecular assemblies is a subject of current interest and has been extensively studied in the literature for rationalizing the structures of both the organic crystals as well as the biomolecules.[35,36] There is now a general consensus that this interaction falling in the moderate energy scale (3–10 kcal $mol^{-1}$) acts to binds molecules together in the crystal. It is likely that this interaction would be used as an important parameter in the design of new solids.[37] As described earlier, the interactions between the acid–acid and the 1,10-phenanthroline–1,10-phenanthroline pairs are isotropic and the interaction between

 

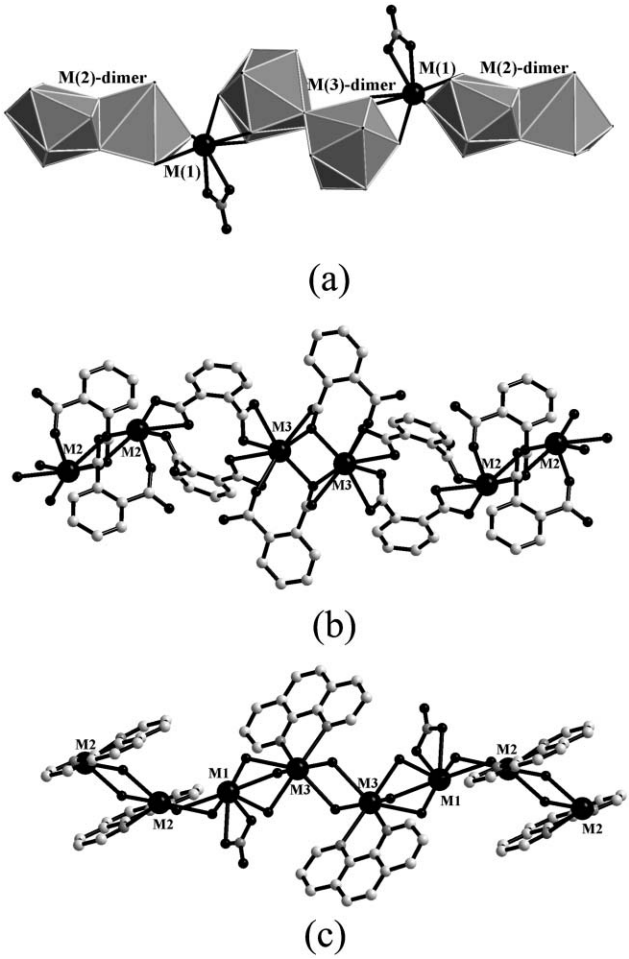


**Fig. 2** (a) The polyhedral connectivity of the M(2) and M(3) dimers and their connectivity to M(1) (see text). (b) Structure shows the connectivity between M(2) and M(3) dimers through acid 3 and acid 4. (c) Structure shows the connectivity involving the secondary ligands with M(1), M(2) and M(3) (1,10-phenanthroline and nitrate).

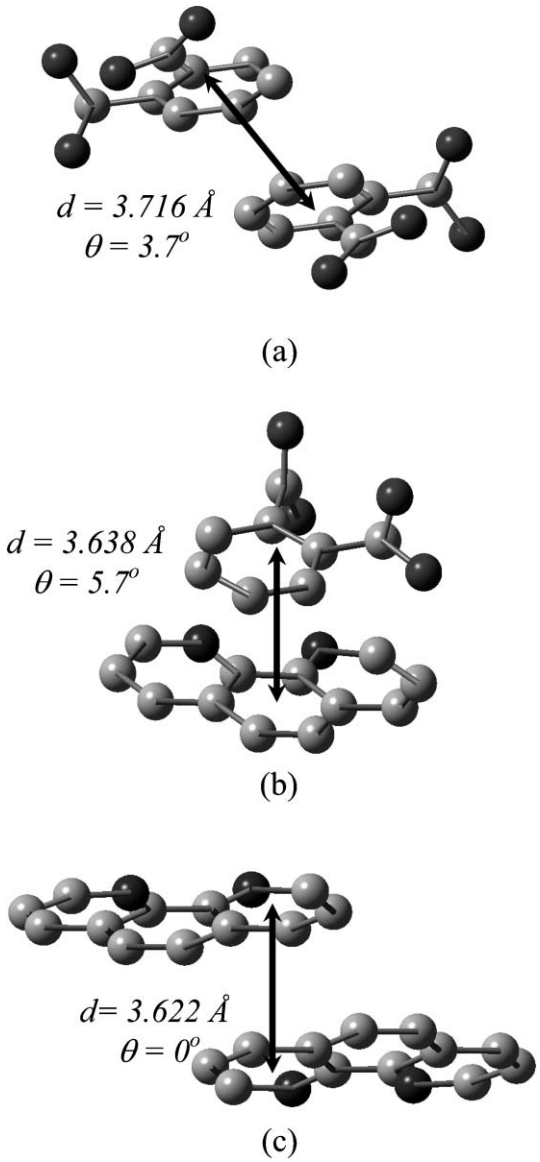


**Fig. 3** The three different types of π···π interactions observed in **I** and **II** (a) acid–acid (b) 1,10-phenanthroline–acid and (c) 1,10-phenanthroline–1,10-phenanthroline.

the acid–1,10-phenanthroline pair is anisotropic. A careful analysis of the π···π interactions in the three systems reveals interesting features. The centroid–centroid distance ($d$) and their inter-planar angles ($\theta$) for the favorable π···π interactions between these rings have been observed for all the three types of interactions with $d$ = 3.716 Å and $\theta$ = 3.7° for the acid–acid pair, $d$ = 3.638 Å and $\theta$ = 5.7° for the 1,10-phenanthroline–1,10-phenanthroline pair and $d$ = 3.622 Å and $\theta$ = 0° for the acid–1,10-phenanthroline pair. From the inter-planar angles ($\theta$), it is clear that the two 1,10-phenanthroline rings are arranged one over the other, but are stacked anti-parallel to each other. This type of anti-parallel arrangement of aromatic rings is commonly observed in systems exhibiting dipolar properties. To understand the role of the various interactions involving the π electrons, we have performed preliminary calculations using the AM1 parameterized Hamiltonian available in the Gausian program suite.[38] AM1 methods, together with a semi-classical dipolar description have been employed recently to establish the relationship between the stability and geometries of organic molecules.[39] The individual molecules are dipolar (dipole moment of the acid as calculated at AM1 level is 7.15 Debye and that for the 1,10-phenanthroline is 2.82 Debye) and the most favorable mode for the arrangement of the two dipolar molecules involve anti-parallel orientation, which cancels the overall dipole moment.[40–42] However, such an arrangement may not be suitable for the anisotropic pair (acid–1,10-phenanthroline) and the overall π-stacked aggregate has a net dipole moment (7.85 Debye).

Using the crystal structure geometry present in **I** and **II**, we have made an evaluation of the strength of the π···π interactions based on single-point energy calculation without the symmetry constraints. The π···π interaction energy was found to be 4.3 kcal mol$^{-1}$, 4.826 kcal mol$^{-1}$ and 5.62 kcal mol$^{-1}$ for the acid–acid, 1,10-phenanthroline–1,10-phenanthroline and acid–1,10-phenanthroline pairs. These energies are in the range comparable to the hydrogen bond energies observed in many solids. The π···π interactions along

with other non-covalent interactions (CH···π and H bond interactions involving the lattice water molecules) possibly lends structural stability to **I** and **II**.

### Optical properties

The lanthanide-centered emission is sensitized by the molecules having π systems. Recently, lanthanide-centered luminescence sensitized by the diketonate type ligands was reported.[43] Férey *et al* reported the luminescence behavior of doped lanthanide carboxylates, which also contains M–O–M one-dimensional chains.[21–23] Since the present compound also has M–O–M chains, we investigated the luminescence behavior of **I** and **II**. In order to investigate the luminescence from the metal center, we have partially doped Eu (2 mol%, **Ia** and 4 mol% **Ib**) and Tb (2 mol%, **Ic** and 4 mol% **Id**) in place of La.

The room temperature photoluminescence properties of all the compounds were studied using an excitation wavelength of 252 nm. The emission spectrum of the pure compounds **I** and **II** show a broad peak centered at ~400 nm (Fig. 4a). This emission may be attributed to the intra ligand luminescence (π* → n or π* → π). Generally, in metal-coordination compounds, the ligand is excited to the singlet state, from where part of the energy is transferred onto the triplet excited state through inter-system crossing (ISC). The triplet exited state then comes to the ground state through radiative emission. This emission also has a competing process called ligand-sensitized energy transfer to the metal center, if the energy levels are favorable.[44,45] This would result in a metal centered luminescence, showing characteristic spectra of the central metal ion. The success of the energy transfer to the metal ion is clearly indicated in the suppression of the intra-ligand emission in the luminescence spectra. A preliminary optical emission of the doped compounds of **I** and **II**, **Ia** (2 mol% Eu), **Ib** (4 mol% Eu), **Ic** (2 mol% Tb) and **Id** (4 mol% Tb) was observed under UV irradiation. As shown in Fig. 4b, very efficient pink/red and green emission is observed for the $Eu^{3+}$ and $Tb^{3+}$ doped samples, respectively.

The room temperature photoluminescence spectra of the Eu and Tb doped samples are given in Fig. 5a and 5b. As can be seen, the main emission band is suppressed followed by the strong red luminescence, characteristics of the $^5D_0 \rightarrow {}^7F_J$ ($J$ = 0, 1, 2, 3, 4) emission bands of the $Eu^{3+}$ ion.[46] The excitation spectrum of **Ia** and **Ib** has a band maximum around 250nm, confirming that the energy transfer takes place from the ligand to $Eu^{3+}$ ion. Under this circumstances, the inter-system crossing (ISC) from the singlet to the triplet excited state of the ligands (1,2-BDC and 1,10-phenanthroline) occurs, followed by the energy transfer to the $^5D_J$, $J$ = 3, 2, 1, 0 state of $Eu^{3+}$ ions (Fig. 5a). A schematic of the various possible energy levels in the doped compounds is given in Fig. 6. In compounds **Ia** and **Ib**, the emission from the $^5D_0 \rightarrow {}^7F_J$ states is responsible for the red/pink luminescence. Thus, the emissions at 580, 543, 615, 650 and 700 nm corresponds to $^5D_0 \rightarrow {}^7F_0$, $^5D_0 \rightarrow {}^7F_1$, $^5D_0 \rightarrow {}^7F_2$, $^5D_0 \rightarrow {}^7F_3$ and $^5D_0 \rightarrow {}^7F_4$ transitions, respectively. In the case of **Ia** (2 mol% Eu) the overall energy transfer is not complete since intra-ligand emission is not quenched fully.[47] For **Ib** (4 mol% Eu), on the other hand, the quenching appears to be more and

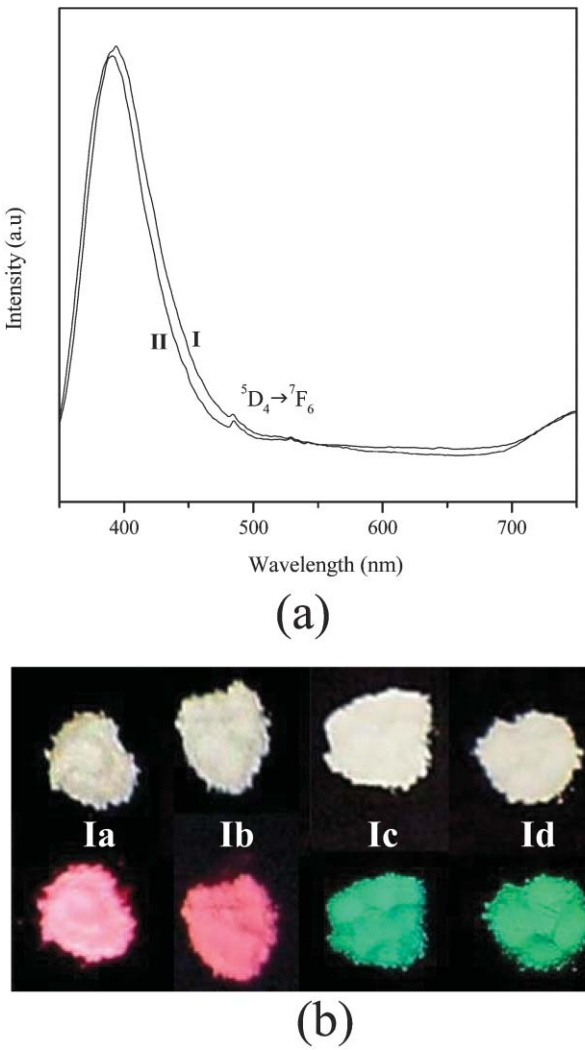


**Fig. 4** (a) Room-temperature photoluminescence spectra for **I** and **II**. (b) Compounds of **Ia**, **Ib**, **Ic**, and **Id** under white (top) and UV (bottom) illuminations.

hence more energy would have been transferred from the ligands. It is likely, that the increased concentration of the $Eu^{3+}$ ions in **Ib** would have resulted in this behavior. This behavior is not expected to be linear as for higher concentrations of $Eu^{3+}$, the metal centered luminescence may be affected by self-quenching.

It has been observed that the emission bands of the $^5D_0 \rightarrow {}^7F_J$ peaks also give an idea about the coordination environment. For example, a ($2J$ + 1) splitting is observed in the emission band for a single type of environment (coordination environment and site symmetry) around the metal ion.[44] In the present case, only one emission band has been observed in the $^5D_0 \rightarrow {}^7F_0$ degenerate transition around 580 nm. This indicates that the Eu(III) ion occupies only one of the three crystallographic sites. Of the three available positions, two are coordinated with 1,10-phenanthroline as a secondary ligand along with the phthalate anions and the remaining site is coordinated to the nitrate and the phthalate anions. The emission at 593 nm corresponds to $^5D_0 \rightarrow {}^7F_1$ transition, which is induced by magnetic dipole moment and is fairly

 

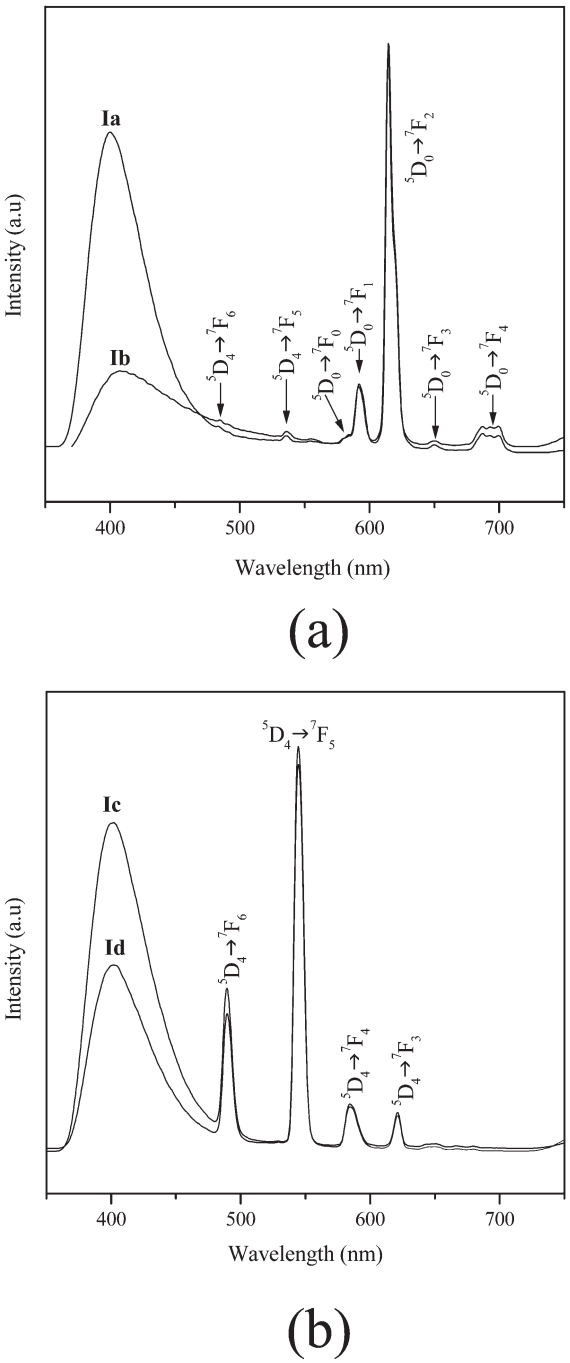


**Fig. 5** Room-temperature photoluminescence spectra of the doped compounds (a) **Ia** (2 mol% Eu) and **Ib** (4 mol% Eu) (b) **Ic** (2 mol% Eu) and **Id** (4 mol% Tb).

insensitive to the coordination environment.[44] The emission at 615nm corresponds to the $^5D_0 \rightarrow {}^7F_2$ transition, which is induced by the electric dipole moment and also sensitive to the environment. At room temperature these are not resolved very well. The intensity ratio, $I(^5D_0 \rightarrow {}^7F_2)/I(^5D_0 \rightarrow {}^7F_1) = \sim 6$, indicates a lower symmetry level of the coordination environment of the $Eu^{3+}$ occupied site.[48] It may be noted that in the present case, the metal ions with CN = 10 is less symmetric than with CN = 8. In **I**, there are two sites, La(1) and La(3), which are 10 coordinated. It is likely that the $Eu^{3+}$ ions occupy

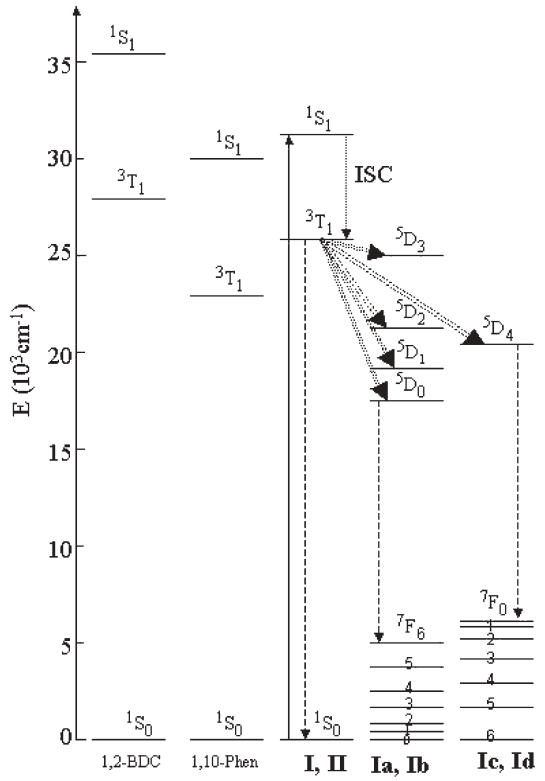


**Fig. 6** Schematic energy level diagram for the pure ligands, **I**, **II** and **Ia–Id** showing the various possible energy transfer processes. (ISC denotes inter-system crossing).

the La(3) sites, which are coordinated by O(8) and N(2) atoms, rather than the La(1) sites, which are completely coordinated by O(10) atoms.

Similarly, in the case of $Tb^{3+}$ doped samples (**Ic** and **Id**), we find a band maximum $\sim$250 nm in the excitation spectrum, indicating that the energy transfer takes place again from the ligand to the $Tb^{3+}$ ions. The emission spectra shows the typical peaks, and the energy transfer occurs from the triplet excited state of the ligand to the $^5D_4$ state of the $Tb^{3+}$ ions.[49] The resultant emission occurs from $^5D_4$ to the $^7F_J$ ($J$ = 3, 4, 5, 6) states giving green luminescence. The various peaks are assigned as follows: $^5D_4 \rightarrow {}^7F_6$ ($\sim$490 nm), $^5D_4 \rightarrow {}^7F_5$ ($\sim$545 nm), $^5D_4 \rightarrow {}^7F_4$ ($\sim$580 nm) and $^5D_4 \rightarrow {}^7F_3$ ($\sim$620 nm) (Fig. 5b). As can be noted, the higher concentration of $Tb^{3+}$ in **Id** shows more quenching of intra-ligand transition giving rise to more intense green emission.

Considering all the four doped compounds, it is becoming obvious that the energy transfer from the ligand to the metal is more pronounced in the $Eu^{3+}$ doped compounds (**Ia** and **Ib**) compared to the $Tb^{3+}$ doped ones (**Ic** and **Id**). It is likely that the availability of more energy levels for $Eu^{3+}$ ($^5D_J$, $J$ = 3, 2, 1, 0) compared to $Tb^{3+}$ ($^5D_4$), would have resulted in the efficient energy transfer. The $^5D_0 \rightarrow {}^7F_2$ ($\sim$615 nm) emission for **Ia** and **Ib** and the $^5D_4 \rightarrow {}^7F_5$ ($\sim$545 nm) emission for **Ic** and **Id**, respectively, correspond to the red and green region of the visible spectrum. The present results are qualitative in nature, and the emission observed in these compounds could be compared to the emissions of the commercial red phosphors (i) $Y_2O_3 : Eu^{3+}$ with 611 nm emission (ii) $(Y,Gd)(P,V)O_4 : Eu^{3+}$

with 615 nm emission and green phosphors (i) $LaPO_4$ : $Ce^{3+}$,$Tb^{3+}$ with 545 nm emission (ii) (Ce,Gd,Tb)$MgB_5O_{10}$ with 542 nm emission (iii) (Ce,Tb)$MgAl_{11}O_{19}$ with 541 nm emission.[49] This opens up a new way of introducing luminescent properties into the hybrid solids with the extended inorganic network structure. In addition, the presence of aromatic linkers with delocalized π electrons (benzene carboxylate and 1,10-phenanthroline) appears to enhance the optical properties.

## Conclusions

The synthesis, structure and characterization of new metal–organic hybrid compounds has been accomplished. The structures are built-up from $MO_{10}$, $MO_6N_2$ and $MO_8N_2$ polyhedral units forming infinite one-dimensional M–O–M chains. The presence of both the nitrate and the carboxylate anions in the same structure is interesting and has been observed for the first time. The $Eu^{3+}$ and $Tb^{3+}$ doped samples, in place of La, show red and green emissions with characteristic transitions resulting from the ligand sensitized energy transfer (or fluorescence resonance energy transfer, FRET). Other similar compounds are currently under investigation to enlarge the field of luminescence in metal–organic hybrid compounds based on rare-earth elements.

## Acknowledgements

SN thanks Department of Science and Technology (DST), Government of India for the award of a research project and AT the Council of Scientific and Industrial Research (CSIR) Government of India, for the award of a research fellowship.

## References

1 N. W. Ocwig, O. D-Friedrichs, M. O'Keeffe and O. M. Yaghi, *Acc. Chem. Res.*, 2005, **38**, 176.
2 G. Férey, *Nat. Mater.*, 2003, **2**, 137.
3 B. Moulton and M. J. Zawarotko, *Chem. Rev.*, 2001, **101**, 1629.
4 B. Moulton, J. Lu, R. Hajndl, S. Hariharan and M. J. Zaworotko, *Angew. Chem., Int. Ed.*, 2002, **41**, 2821.
5 J. S. Seo, D. Whang, H. Lee, S. I. Jun, J. Oh, Y. J. Jeon and K. Kim, *Nature*, 2000, **404**, 982.
6 R. Kitaura, K. Fujimoto, S. Noro, M. Kono and S. Kitagawa, *Angew. Chem., Int. Ed.*, 2002, **41**, 133.
7 N. L. Rosi, J. Eukert, M. Eddaoudi, D. T. Vodak, J. Kim, M. O'Keeffe and O. M. Yaghi, *Science*, 2003, **300**, 1127.
8 K. Barthelet, J. Marrot, G. Férey and D. Riou, *Chem. Commun.*, 2004, 520.
9 X. Zhao, B. Xiao, A. J. Fletcher, K. M. Thomas, D. Bradshaw and M. J. Rosseinsky, *Science*, 2003, **306**, 1012.
10 C. N. R. Rao, S. Natarajan and R. Vaidhyanathan, *Angew. Chem., Int. Ed.*, 2004, **43**, 1466.
11 A. Thirumurugan and S. Natarajan, *Dalton Trans.*, 2004, 2923.
12 A. Thirumurugan and S. Natarajan, *Solid State Sci.*, 2004, 599.
13 A. Thirumurugan and Srinivasan Natarajan, *Chem. Eur. J.*, 2004, 762.
14 O. M. Yaghi, M. O'Keeffe, N. W. Ockwig, H. K. Chae, M. Eddaoudi and J. Kim, *Nature*, 2003, **423**, 705.
15 M. Eddaoudi, J. Kim, D. Vodak, A. Sudik, J. Wachfer, M. O'Keeffe and O. M. Yaghi, *Proc. Natl. Acad. Sci. USA*, 2002, **99**, 4900.
16 W. Chen, J. Y. Wang, C. Chen, Q. Yue, H. M. Yuan, J. S. Chen and S. N. Wang, *Inorg. Chem.*, 2003, **42**, 944.
17 C-M. Wang, S-T. Chuang, Y-L. Chuang, H-M. Kao and K-H. Lii, *J. Solid State Chem.*, 2004, **177**, 1257.
18 C. Serre, J. Marrot and G. Férey, *Inorg. Chem.*, 2005, **44**, 654.
19 C. Serre, F. Millange, J. Marrot and G. Férey, *Chem. Mater.*, 2002, **14**, 2409.
20 C. Serre and G. Férey, *J. Mater. Chem.*, 2002, **12**, 3053.
21 C. Serre, F. Pelle, N. Gardant and G. Férey, *Chem. Mater.*, 2004, **16**, 1177.
22 F. Millange, C. Serre, J. Marrot, N. Gardant, F. Pelle and G. Férey, *J. Mater. Chem.*, 2004, **14**, 642.
23 C. Serre, F. Millange, C. Thouvenot, N. Gardant, F. Pelle and G. Férey, *J. Mater. Chem.*, 2004, **14**, 1530.
24 C. Serre, N. Stock, T. Bein and G. Férey, *Inorg. Chem.*, 2004, **43**, 3159.
25 Y. Wan, L. Zhang, L. Jin, S. Cao and S. Lu, *Inorg. Chem.*, 2003, **42**, 4985.
26 Y-B. Wang, X-J. Zheng, W. J. Zhuang and L-P. Jin, *Chem. Eur. J.*, 2003, 1355.
27 Y. Wan, L. Jin, K. Wang, L. Zhang, X. Zheng and S. Lu, *New J. Chem.*, 2002, **26**, 1590.
28 J-L. Song, C. Lei and J-G. Mao, *Inorg. Chem.*, 2004, **43**, 5630.
29 D. Sendor, M. Hilder, T. Juestel, P. C. Junk and U. H. Kyanast, *New J. Chem.*, 2003, **27**, 1070.
30 H. K. Fun, S. S. S. Raj, R. G. Xiong, J. L. Zuo, Z. Yu and X. Z. You, *J. Chem. Soc., Dalton Trans.*, 1999, 1915.
31 O. R. Evans, R. G. Xiong, Z. Wang, G. K. Wong and W. Lin, *Angew. Chem., Int. Ed.*, 1999, **38**, 536.
32 D. Sun, R. Cao, Y. Liang, Q. Shi, W. Su and M. Hong, *J. Chem. Soc., Dalton Trans.*, 2001, 2335.
33 G. M. Sheldrick, *SADABS Siemens Area Detector Absorption Correction Program*, University of Göttingen, Gottingen, Germany, 1994.
34 G. M. Sheldrick, *SHELXTL-PLUS Program for Crystal Structure Solution and Refinement*, University of Gottingen, Gottingen, Germany, 1997.
35 C. A. Hunter, *Chem. Soc. Rev.*, 1994, **23**, 101.
36 C. A. Hunter, K. R. Lawson, J. Perkins and C. J. Urch, *J. Chem. Soc., Perkin Trans. 2*, 2001, 651.
37 J. D. Dunitz and A. Gavezzotti, *Angew. Chem., Int. Ed.*, 2005, **44**, 1766–1786.
38 Gaussian 03, Revision B.05, M. J. Frisch, G. W. Trucks, H. B. Schlegel, G. E. Scuseria, M. A. Robb, J. R. Cheeseman, J. A. Montgomery, Jr., T. Vreven, K. N. Kudin, J. C. Burant, J. M. Millam, S. S. Iyengar, J. Tomasi, V. Barone, B. Mennucci, M. Cossi, G. Scalmani, N. Rega, G. A. Petersson, H. Nakatsuji, M. Hada, M. Ehara, K. Toyota, R. Fukuda, J. Hasegawa, M. Ishida, T. Nakajima, Y. Honda, O. Kitao, H. Nakai, M. Klene, X. Li, J. E. Knox, H. P. Hratchian, J. B. Cross, C. Adamo, J. Jaramillo, R. Gomperts, R. E. Stratmann, O. Yazyev, A. J. Austin, R. Cammi, C. Pomelli, J. W. Ochterski, P. Y. Ayala, K. Morokuma, G. A. Voth, P. Salvador, J. J. Dannenberg, V. G. Zakrzewski, S. Dapprich, A. D. Daniels, M. C. Strain, O. Farkas, D. K. Malick, A. D. Rabuck, K. Raghavachari, J. B. Foresman, J. V. Ortiz, Q. Cui, A. G. Baboul, S. Clifford, J. Cioslowski, B. B. Stefanov, G. Liu, A. Liashenko, P. Piskorz, I. Komaromi, R. L. Martin, D. J. Fox, T. Keith, M. A. Al-Laham, C. Y. Peng, A. Nanayakkara, M. Challacombe, P. M. W. Gill, B. Johnson, W. Chen, M. W. Wong, C. Gonzalez and J. A. Pople, Gaussian Inc., Pittsburgh PA, 2003.
39 P. Mahatha and S. Natarajan, *Eur. J. Inorg. Chem.*, 2004, 762.
40 M. J. S. Dewar, E. G. Zoebisch, E. F. Healy and J. J. P. Stewart, *J. Am. Chem. Soc.*, 1985, **107**, 3902.
41 A. J. Stone, *The Theory of Intermolecular Forces*, Cladrendon Press, Oxford, 1996.
42 A. Datta and S. K. Pati, *J. Chem. Phys.*, 2003, **118**, 8420.
43 A. P. Bassett, S. W. Magennis, P. B. Glover, D. J. Lewis, N. Spencer, S. Parsons, R. M. Williams, L. D. Cola and Z. Pikramenou, *J. Am. Chem. Soc.*, 2004, **126**, 9413.
44 J.-C. G. Bunzli and G. R. Choppin, *Lanthanide Probes in Life, Chemical and Earth Sciences. Theory and Practice*, Elsevier, Amsterdam, 1989.
45 P. R. Selvin, *Nat. Struct. Biol.*, 2000, **7**, 730.
46 N. Sabbatini, M. Guardigli and J-M. Lahn, *Coord. Chem. Rev.*, 1993, **123**, 201.
47 F. S. Richardson, *Chem. Rev.*, 1982, **82**, 541.
48 S. L. Murov, I. Carmicael and G. L. Hug, *Handbook of Photochemistry*, Marcel Dekker, New York, 1993.
49 G. Blasse and B. C. Grabmaier, *Luminescent Materials*, Springer, Berlin, 1994.

 